Arch Appl Mech (2010) 80: 201–215
DOI 10.1007/s00419-009-0311-4

ORIGINAL

M. Talebitooti · M. Ghayour · S. Ziaei-Rad · R. Talebitooti

Free vibrations of rotating composite conical shells with stringer and ring stiffeners

Received: 29 October 2008 / Accepted: 25 February 2009 / Published online: 19 March 2009

Abstract In this paper, an analytical solution for the free vibration of rotating composite conical shells with axial stiffeners (stringers) and circumferential stiffener (rings), is presented using an energy-based approach. Ritz method is applied while stiffeners are treated as discrete elements. The conical shells are stiffened with uniform interval and it is assumed that the stiffeners have the same material and geometric properties. The study includes the effects of the coriolis and centrifugal accelerations, and the initial hoop tension. The results obtained include the relationship between frequency parameter and circumferential wave number as well as rotating speed at various angles. Influences of geometric properties on the frequency parameter are also discussed. In order to validate the present analysis, it is compared with other published works for a non-stiffened conical shell; other comparison is made in the special case where the angle of the stiffened conical shell goes to zero, i.e., stiffened cylindrical shell. Good agreement is observed and a new range of results is presented for rotating stiffened conical shells which can be used as a benchmark to approximate solutions.

Keywords Rotating composite laminated conical shells · Stringer/ring stiffener · Natural Frequency · Energy method

1 Introduction

Circular and conical shell structures are increasingly being used in many engineering applications. Vibration of shell structure has been extensively studied [1–3]. Rotating conical shells are being widely used in the drive shafts of gas turbines, high-speed centrifugal separators, motors, and rotor systems.

Chen et al. [4] applied the finite-element method for rotating conical shells. Although rotating shells of revolution are increasingly being used in many industries, most studies were restricted to the vibration analysis of rotating cylindrical shells. They include the works by Lam on the rotating composite and sandwich-type cylindrical shells [5,6] as well as a comparison study on different thin shell theories and also a discussion on influence of boundary condition for rotating cylindrical shell [7,8]. Lam and Hua [9] analyzed the free vibration of rotating circular conical shell. Zhao et al. [10] presented the free vibration analysis of simply supported rotating cross-ply laminated cylindrical shells with axial and circumferential stiffeners, using an energy approach. The effects of these stiffeners were evaluated via two methods: stiffeners treated as discrete element; and with the properties of the stiffeners averaged over the shell surface by the smearing method. Jafari and Bagheri investigated the free vibration analysis of simply supported rotating cylindrical shells with

M. Talebitooti (✉) · M. Ghayour · S. Ziaei-Rad
Department of Mechanical Engineering, Isfahan University of Technology, 84156-83111 Isfahan, Iran
E-mail: mt_talebi@me.iut.ac.ir
Tel.: 0098-311-3915247

R. Talebitooti
Department of Mechanical Engineering, Iran University of Science & Technology, 16844 Tehran, Iran

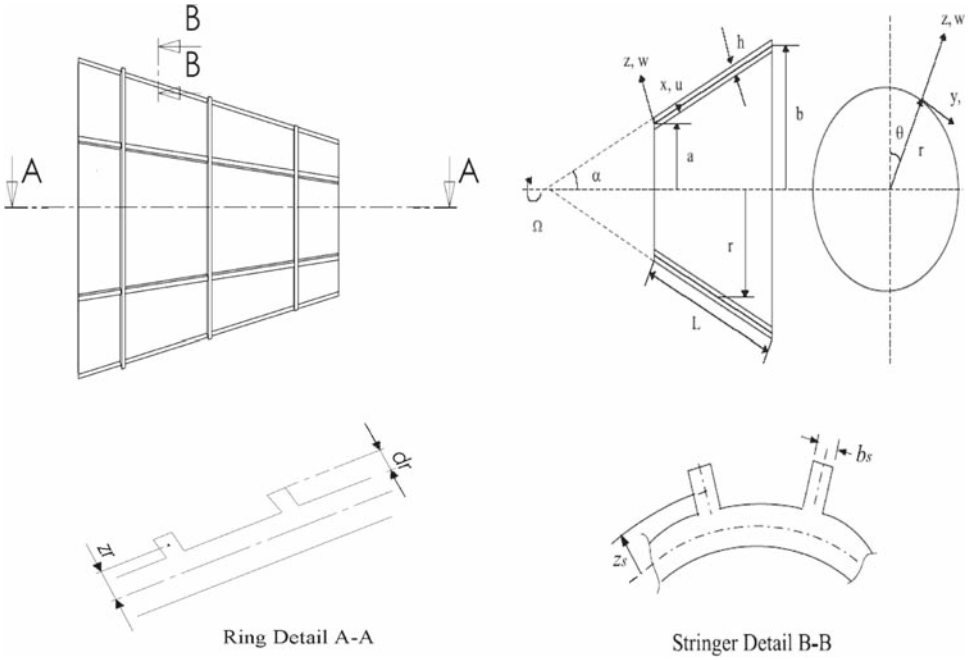

Fig. 1 Geometry of the stiffened rotating laminated conical shell

circumferential stiffeners, i.e., rings with non-uniform stiffeners eccentricity and non-uniform stiffeners spacing distribution [11]. A few studies concerning free vibration analysis of conical shells have been carried out, namely by Lim and Liew [12].

All the pervious studies dealt with only stiffened rotating cylindrical shell or rotating non-stiffened conical shell. In the present study, an energy-based method is formulated to determine the effects of circumferential wave number, number of stiffener, geometry of shell and rotating speed on the frequency characteristic of stiffened rotating cross-ply laminated conical shells. Ritz method is applied while stiffeners are treated as discrete method. Imposing the given boundary condition, the numerical eigenvalue equation for the free vibration of the rotating composite conical shell are derived and then solved. Based on the eigensolution, results are obtained to discuss the material orthotropic influence on the frequency characteristics. Variations of frequency parameter with circumferential wave number are also studied for different rotating velocities as well as the effects of number of stiffener on the frequency characteristics is investigated. By comparing with the results available in the literature for the cases of stiffened rotating composite cylindrical shells and the non-stiffened rotating composite conical shells, the accuracy of the present analysis is validated.

2 Theoretical formulation

The main emphasis of the analysis to determine the global response of the laminated component, for example, fundamental vibration frequencies, and associated mode shapes, can often be accurately determined using relatively simple equivalent single-layer laminated theories (ESL theories), especially for thin laminated shell. The stiffened conical shell, as shown in Fig. 1, is considered to be thin, laminated, and composed of an arbitrary number layers. In this figure, α is the half-cone angle, L the length, h the thickness, a and b the radii at two ends, and Ω is the constant angular velocity of conical shell about its symmetrical and horizontal axis. The reference surface of the conical shell is taken to be at its middle surface where an orthogonal co-ordinate system (x, θ, z) is fixed, and $r_x = r_x(x)$ is a radius at any co-ordinate point (x, θ, z). The displacement of the shell in the x, θ and z directions are denoted by u, v, w, respectively. The depth and width of the stiffeners are symbolized by d_s (or $_r$), b_s (or $_r$). Subscripts (s, r) indicate the stringer and ring stiffeners, respectively. The displacement from the middle surface of shell to the centroid of the stringer and ring are denoted by z_s and z_r, respectively.

The strain energy for the composite conical shell is expressed as

$$U_\varepsilon = \frac{1}{2}\int_0^L \int_0^{2\pi} \varepsilon^T [\mathrm{S}]\varepsilon R \mathrm{d}\theta \mathrm{d}x \tag{1}$$

where [S] is the stiffness matrix and the strain vector ε can be written as

$$\varepsilon^T = \left\{ e_1 \; e_2 \; \gamma \; \kappa_1 \; \kappa_2 \; 2\tau \right\} \tag{2}$$

where symbols e_1, e_2, and γ are middle surface strains and symbols κ_1, κ_2, and τ are middle surface curvatures (the subscripts 1 and 2 denote the meridional x and circumferential θ directions). The geometric relations of deformations for the reference surface of the conical shell can be written as

$$\begin{aligned}
e_1 &= \frac{\partial u}{\partial x} \quad e_2 = \frac{1}{r_x}\frac{\partial v}{\partial \theta} + \frac{u\sin\alpha + w\cos\alpha}{r_x} \quad e_{12} = \frac{1}{r_x}\frac{\partial u}{\partial \theta} + \frac{\partial v}{\partial x} - \frac{v\sin\alpha}{r_x} \\
\kappa_1 &= -\frac{\partial^2 w}{\partial x^2} \quad \kappa_2 = -\frac{1}{r_x^2}\frac{\partial^2 w}{\partial \theta^2} + \frac{\cos\alpha}{r_x^2}\frac{\partial v}{\partial \theta} - \frac{\sin\alpha}{r_x}\frac{\partial w}{\partial x} \\
\tau &= -\frac{1}{r_x}\frac{\partial^2 w}{\partial x \partial \theta} + \frac{\sin\alpha}{r_x^2}\frac{\partial w}{\partial \theta} + \frac{\cos\alpha}{r_x}\frac{\partial v}{\partial x} - \frac{v\sin\alpha\cos\alpha}{r_x^2}
\end{aligned} \tag{3}$$

It is assumed that the displacements are continuous functions of the thickness coordinate. This results in continuous transverse strains.

And the stiffness matrix [S] for a cross-ply laminated shell is given by

$$[\mathrm{S}] = \begin{bmatrix}
A_{11} & A_{12} & A_{16} & B_{11} & B_{12} & B_{16} \\
A_{21} & A_{22} & A_{26} & B_{21} & B_{22} & B_{26} \\
A_{61} & A_{62} & A_{66} & B_{61} & B_{62} & B_{66} \\
B_{11} & B_{12} & B_{16} & D_{11} & D_{12} & D_{16} \\
B_{21} & B_{22} & B_{26} & D_{21} & D_{22} & D_{26} \\
B_{61} & B_{62} & B_{66} & D_{61} & D_{62} & D_{66}
\end{bmatrix} \tag{4}$$

where $A = [A_{ij}]$, $B = [B_{ij}]$, and $D = [D_{ij}]$ $(i, j = 1, 2, 6)$ are extensional, coupling, and bending stiffness matrixes. For an arbitrarily laminated composite shell, they can be rewritten as

$$\begin{aligned}
A_{ij} &= \sum_{k=1}^{N} \bar{Q}_{ij}^k (h_k - h_{k+1}) \\
B_{ij} &= \frac{1}{2}\sum_{k=1}^{N} \bar{Q}_{ij}^k (h_k^2 - h_{k+1}^2) \\
D_{ij} &= \frac{1}{3}\sum_{k=1}^{N} \bar{Q}_{ij}^k (h_k^3 - h_{k+1}^3)
\end{aligned} \tag{5}$$

where N is the number of total layers of the laminated composite conical shell. Parameters h_k and h_{k+1} denote the distance from the shell reference surface to the outer and inner surface of the kth layer as shown in Fig. 2. $\bar{Q}_{ij}^k$ is the element of the transformed reduced stiffness matrix for the kth layer defined as

$$\bar{Q}^k = P^{-1} Q^k P \tag{6}$$

where [P] is the transformation matrix for the principal material coordinate and the shell coordinate system and is defined as

$$[\mathrm{P}] = \begin{bmatrix}
\cos^2\beta & \sin^2\beta & 2\cos\beta\sin\beta \\
\sin^2\beta & \cos^2\beta & -2\cos\beta\sin\beta \\
-\cos\beta\sin\beta & \cos\beta\sin\beta & \cos^2\beta - \sin^2\beta
\end{bmatrix} \tag{7}$$

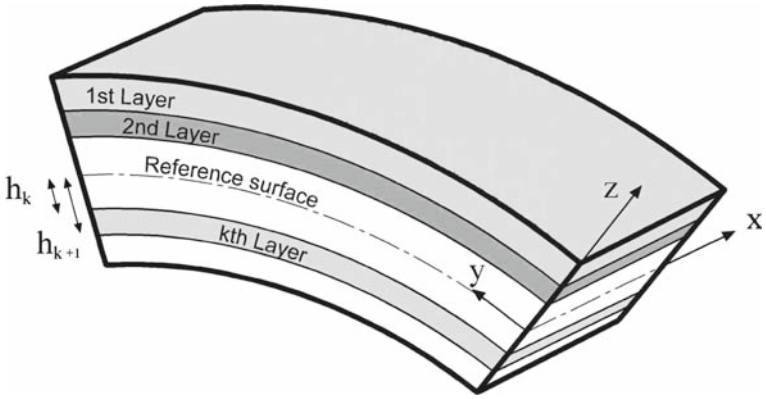

Fig. 2 Cross-sectional view of the laminated conical shell

where β is the orientation of the fibers and [Q] is reduced stiffness matrix defined as

$$[Q] = \begin{bmatrix} Q_{11} & Q_{12} & 0 \\ Q_{21} & Q_{22} & 0 \\ 0 & 0 & Q_{66} \end{bmatrix} \tag{8}$$

and the material constants in the reduced stiffness matrix [Q] defined as

$$\begin{aligned} Q_{11} &= \frac{E_{11}}{1-\upsilon_{12}\upsilon_{21}}, \quad Q_{12} = Q_{21} = \frac{\upsilon_{12}E_{22}}{1-\upsilon_{12}\upsilon_{21}}, \\ Q_{22} &= \frac{E_{22}}{1-\upsilon_{12}\upsilon_{21}}, \quad Q_{66} = G_{12} \end{aligned} \tag{9}$$

where E_{11} and E_{22} are the elastic modules, G_{12} the shear modulus, and υ_{12} and υ_{21} the Poisson's ratios.

We should define the work carried out on the shell due to the centrifugal force generated by rotation. The work done on the shell can be written as

$$U_h = \frac{1}{2}\int_0^L \int_0^{2\pi} N_\theta \left[\frac{1}{r_x}\frac{\partial v}{\partial \theta} + \frac{u\sin\alpha + w\cos\alpha}{r_x}\right]^2 r_x \mathrm{d}x\mathrm{d}\theta \tag{10}$$

where N_θ is the initial hoop stress due to centrifugal force and defined as

$$N_\theta = \rho h \Omega^2 r_x^2(x) \tag{11}$$

where $r_x(x) = a + x\sin\alpha$.

The kinetic energy of the rotating conical shell is expressed as

$$T = \frac{1}{2}\rho h \int_0^{2\pi}\int_0^L \vec{V}.\vec{V} r_x \mathrm{d}x\mathrm{d}\theta \tag{12}$$

where $\vec{V}$ is the velocity vector at any point of the shell and given by

$$\vec{V} = \dot{\vec{r}} + \left(\Omega\cos\alpha\vec{i} - \Omega\sin\alpha\vec{k}\right) \times \vec{r} \tag{13}$$

Here $(\cdot)$ presents differentiation with respect to time.

In Eq. (13) the displacement vector is written as

$$\vec{r} = u\vec{i} + v\vec{j} + w\vec{k} \tag{14}$$

where $\vec{i}$, $\vec{j}$ and $\vec{k}$, respectively, denote the unit vectors in the x, θ, and z directions in the nonrotating frame.

The stiffeners (rings and stringers) are assumed to be an integral part of the shell and have been directly included in the analysis. In order to maintain displacement compatibility between the stiffeners and the stiffened shell, a special transformation is used here. The transformation includes coupling effects due to the eccentric stiffener placement. It should be also noted that the displacements vary through the stiffeners depth. Therefore, the displacement of a point at distance z from the shell middle surface for the stiffeners can be expressed by shell displacement function.

$$u_s = u - z\frac{\partial w}{\partial x}, \quad v_s = v - \frac{z}{R}\frac{\partial w}{\partial \theta}, \quad w_s = w \tag{15}$$

The strain of the stringers in the meridional direction and the strain of the rings in the circumferential direction are defined as

$$\varepsilon_{sx} = \frac{\partial u}{\partial x} - z\frac{\partial^2 w}{\partial x^2} \tag{16}$$

$$\varepsilon_{r\theta} = \frac{1}{r_x}\left(\frac{\partial v}{\partial \theta} - \frac{z}{r_x}\frac{\partial^2 w}{\partial \theta^2} + u\sin\alpha - z\sin\alpha\frac{\partial w}{\partial x} + w\cos\alpha\right) \tag{17}$$

Using the discrete stiffener theory, the strain energy for the stringer can be written as

$$U_s = \frac{1}{2}\sum_{k=1}^{N_s} E_{sk}\int_0^L\int_{A_{sk}} \varepsilon_{sx}^2 \mathrm{d}A_{sk}\mathrm{d}x + \frac{1}{2}\sum_{k=1}^{N_s} G_{sk}J_{sk}\int_0^L\left[\frac{1}{r_{xk}^2}\left(\frac{\partial^2 w_s}{\partial\theta\partial x}\right)^2\right]\mathrm{d}x \tag{18}$$

where $G_{sk}J_{sk}$, and A_{sk} are the torsional stiffness and the cross sectional area of the kth stringer, respectively, and N_s is the number of stringer.

For the ring, the strain energy can be written as

$$U_r = \frac{1}{2}\sum_{k=1}^{N_r} E_{rk}\int_0^{2\pi}\int_{A_{rk}} \varepsilon_{r\theta}^2 \mathrm{d}A_{rk}\mathrm{d}x + \frac{1}{2}\sum_{k=1}^{N_r} G_{rk}J_{rk}\int_0^{2\pi}\left[\frac{1}{r_{xk}^2}\left(\frac{\partial^2 w_s}{\partial\theta\partial x}\right)^2\right] r_{xk}\mathrm{d}\theta \tag{19}$$

where $G_{rk}J_{rk}$ and A_{rk} are the torsional stiffness and the cross sectional area of the kth ring, respectively, and N_s is the number of stringer.

Next, the kinetic energy for the stringers and rings may be written as

$$T_s = \frac{1}{2}\rho_{sk}\sum_{k=1}^{N_s}\int_0^L\int_{A_{sk}}\left[\begin{array}{l}\dot{u}_s^2 + \dot{v}_s^2 + \dot{w}_s^2 + \Omega^2 v_s^2 + 2\Omega\sin\alpha\,(\dot{v}_s u_s - \dot{u}_s v_s)\\ \quad + 2\Omega\cos\alpha\,(\dot{v}_s w_s - \dot{w}_s v_s) + \Omega^2\,(w_s\cos\alpha + u_s\sin\alpha)\end{array}\right]\mathrm{d}A_{sk}\mathrm{d}x \tag{20}$$

$$T_r = \frac{1}{2}\rho_{sk}\sum_{k=1}^{N_r}\int_0^{2\pi}\int_{A_{rk}}\left[\begin{array}{l}\dot{u}_r^2 + \dot{v}_r^2 + \dot{w}_r^2 + \Omega^2 v_r^2 + 2\Omega\sin\alpha\,(\dot{v}_r u_r - \dot{u}_r v_r)\\ \quad + 2\Omega\cos\alpha\,(\dot{v}_r w_r - \dot{w}_r v_r) + \Omega^2\,(w_r\cos\alpha + u_r\sin\alpha)\end{array}\right] r_{xk}\mathrm{d}A_{rk}\mathrm{d}\theta \tag{21}$$

where $\rho_{s(orr)k}$ is the density of the kth stringer (or ring).

In the case of stringer, the hoop stress is not presented by centrifugal force, but the work done on the ring is similar to that of shell. Therefore, the work expressions for the stringer and ring are

$$U_{sh} = 0 \tag{22}$$

$$U_{rh} = \frac{1}{2}\sum_{k=1}^{N_r}\int_0^{2\pi}\int_{A_{rk}} N_\theta\left[\frac{1}{r_{xk}}\frac{\partial v_r}{\partial\theta} + \frac{u_r\sin\alpha + w_r\cos\alpha}{r_{xk}}\right]^2 r_{xk}\mathrm{d}A_{rk}\mathrm{d}\theta \tag{23}$$

The considered conical shell is simply supported at both meridional ends. The mathematical expression for this boundary condition are given by

$$v = w = M_x = N_x = 0 \quad at \quad x = 0, L \tag{24}$$

Table 1 The geometrical parameters and material properties of the stiffeners used in the present study

Stiffener type	Stringer	Ring
Depth (mm)	8	8
Width (mm)	2	2
E (N/m^2)	$3.0E_{11}$	$3.0E_{11}$
υ	0.3	0.3
$\rho(kg/m^3)$	1643	1643

The admissible displacement functions satisfying the boundary condition have the following forms:

$$\begin{aligned} u &= U\cos(\lambda x)\left[\cos(n\theta)\cos(\omega t) - \sin(n\theta)\sin(\omega t)\right] \\ v &= V\sin(\lambda x)\left[\sin(n\theta)\cos(\omega t) + \cos(n\theta)\sin(\omega t)\right] \\ w &= W\sin(\lambda x)\left[\cos(n\theta)\cos(\omega t) - \sin(n\theta)\sin(\omega t)\right] \end{aligned} \tag{25}$$

where $\lambda = \frac{m\pi}{L}$ and U, V, W are the amplitudes for each direction and ω is the natural frequency.

Therefore, the energy functional of stiffened rotating composite conical shell can be written as

$$\Pi = T + T_r + T_s - U_h - U_\varepsilon - U_s - U_r - U_{rh} \tag{26}$$

Substituting Eq. (25) into Eq. (26) and then applying Hamilton's principle to the energy functional yields the following matrix relationship [13]

$$\begin{bmatrix} L_{11} & L_{12} & L_{13} \\ L_{21} & L_{22} & L_{23} \\ L_{31} & L_{32} & L_{33} \end{bmatrix} \begin{Bmatrix} U \\ V \\ W \end{Bmatrix} = 0 \tag{27}$$

where the coefficients $L_{ij}(i, j = 1, 2, 3)$ are given in detail in Appendix A.

For convenience in solving of eigenvalue equation, rewriting resulting according to ω, the eigenvalue equation is obtained on following matrix form,

$$[H_1\omega^2 + H_2\omega + H_3]d = 0 \tag{28}$$

where $d = [\,U\ V\ W\,]'$.

Equation (28) is a non-standard eigenvalue equation. For a given frequency, it can be transformed equivalently into a standard form of eigenvalue equation as

$$\left(\begin{bmatrix} 0 & I \\ -H_3 & -H_2 \end{bmatrix} - \begin{bmatrix} I & 0 \\ 0 & H_1 \end{bmatrix}\omega\right) \begin{Bmatrix} d \\ \omega d \end{Bmatrix} = 0 \tag{29}$$

where I is the 3×3 identity matrix.

Using a conventional eigenvalue approach, the standard eigenvalue equation (29) can be solved and six eigenvalues for ω_i are obtained. From these eigenvalues, the two real eigenvalues, one positive and the other negative, whose absolute values are the smallest, are chosen. These two eigenvalues are the eigensolution, and they correspond, respectively, to the backward- and forward-traveling waves.

3 Numerical result

The geometrical dimensions and material properties of the stiffeners used in the present study are given in Table 1. To check the validity of the present analysis, three comparisons are made with results in the literature. The first comparison, as shown in Table 2, is for a non-stiffened non-rotating conical shell. The second, Fig. 3, is for a non-rotating stiffened cylindrical shell by taking $\alpha = 0$ into the present formulations. The last comparisons as shown in Fig. 4, is for rotating stiffened cylindrical shell by taking $\alpha = 0$ into the present formulations. In these three comparisons, shells have simply supported boundary conditions in the both ends.

The above comparisons show very good agreement between the present computed results and those in the literature and thus indicate the accuracy of the present work. In all of the results, the lamination scheme is $[0°/90°/0°]$, the shell material property parameters used are $E_{11}/E_{22} = 2.5$ and $\upsilon_{12} = 0.26$, and $\rho = 1{,}643\,(kg/m^3)$.

Table 2 Comparison of the frequency parameter $f = \omega b\sqrt{((1-\upsilon^2)\rho/E)}$ for the free vibration of non-rotating truncated circular conical shell with simply supported boundary condition

n	$\alpha = 30°$		$\alpha = 45°$		$\alpha = 60°$	
	Present study	[14]	Present study	[14]	Present study	[14]
1	0.9142	–	0.7604	–	0.5411	–
2	0.8309	0.8324	0.7243	0.7264	0.5238	0.5255
3	0.7231	0.7234	0.6715	0.6728	0.4974	0.4987
4	0.6137	0.6132	0.6098	0.6103	0.4648	0.4656
5	0.5148	0.5141	0.5457	0.5457	0.4287	0.4292
6	0.4310	0.4304	0.4840	0.4837	0.3919	0.3921
7	0.3622	0.3620	0.4274	0.4271	0.3560	0.3561
8	0.3068	0.3070	0.3771	0.3769	0.3223	0.3225
9	0.2626	0.2634	0.3332	0.3333	0.2915	0.2919

($m = 1$, $\upsilon = 0.3$, $h/b = 0.001$, $\text{Lsin}\alpha/b = 0.25$, $E_{11} = E_{22} = 7.6 \times 10^9$, $G_{12} = 4.1 \times 10^9$)

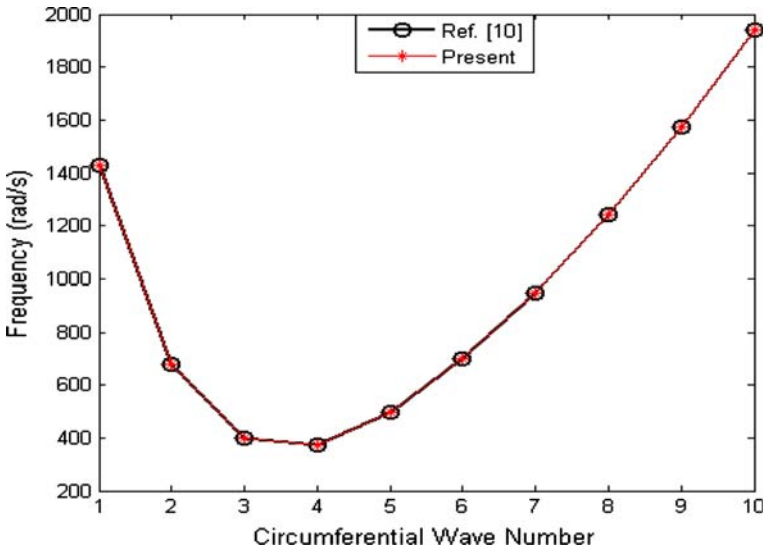

Fig. 3 Variation of the natural frequencies for the non-rotating and orthogonally stiffened composite cylindrical shell with the circumferential wave number. Comparison of results from present study with those reported in [10]

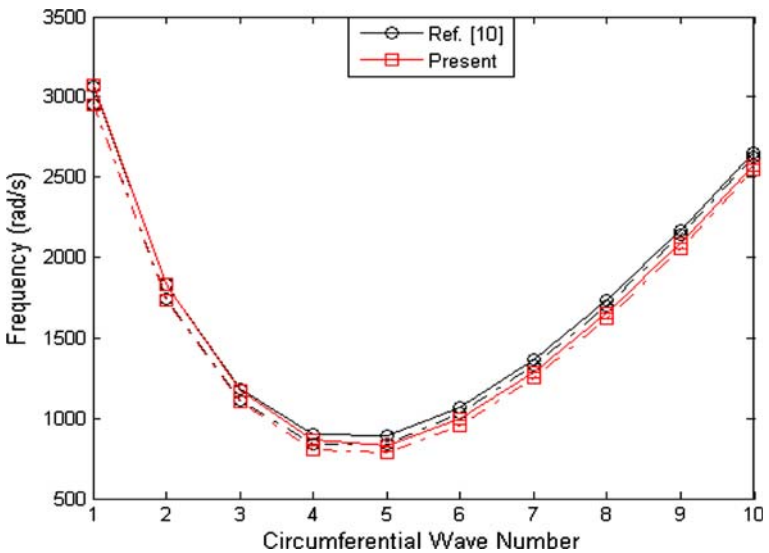

Fig. 4 Variation of the natural frequencies for the rotating and orthogonally stiffened composite cylindrical shell with the circumferential wave number. Comparison of results from present study with those reported in [10]

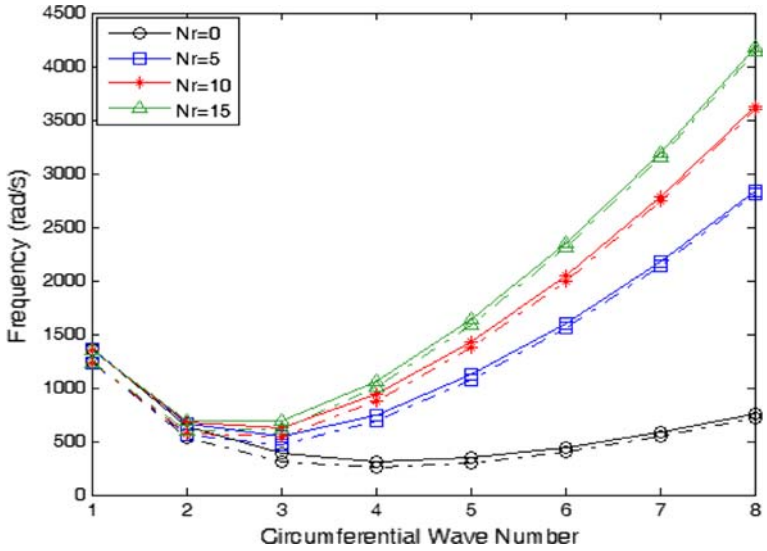

Fig. 5 Variation of the natural frequencies for the rotating and ring stiffened composite conical shell with the circumferential wave number at various different numbers of rings. Lamination scheme [0°/90°/0°], $L/a = 8$, $h/a = 0.008$, $m = 1$, $N_s = 0$, $\Omega = 10$(rev/s), $\alpha = 5°$

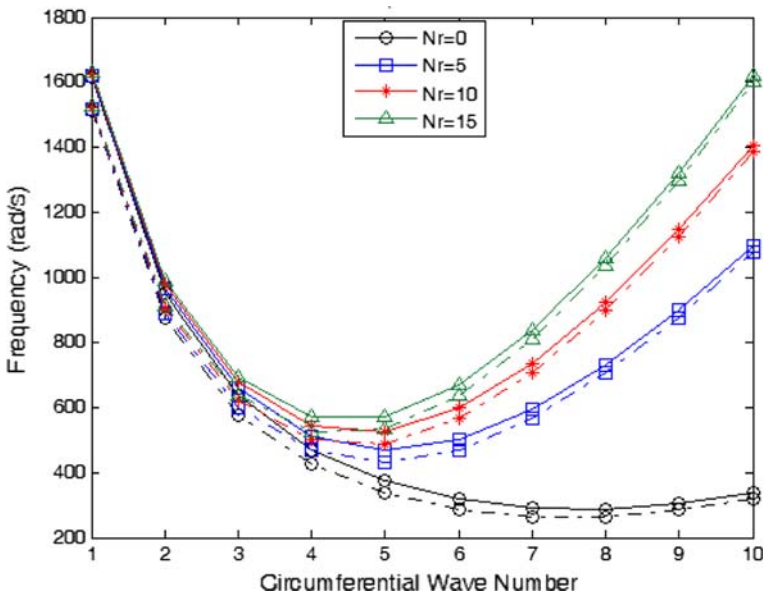

Fig. 6 Variation of the natural frequencies for the rotating and ring stiffened composite conical shell with the circumferential wave number at various different numbers of rings. Lamination scheme [0°/90°/0°], $L/a = 8$, $h/a = 0.008$, $m = 1$, $N_s = 0$, $\Omega = 10$(rev/s), $\alpha = 30°$

Figures 5 and 6, respectively, illustrate the effects of the number of rings on the frequencies of the stiffened rotating conical shell with different cone angles, namely, $\alpha = 5°$ and 30°. In these cases, the number of the stringers is 0. From the figures it can be observed that, at small circumferential wave number, i.e., n equal to 1 and 2, influence of number of rings is insignificant. At large circumferential wave number n, the frequency increases with number of rings, and the increasing gradient becomes small with the increase in the number of rings. However, it is also seen from Figs. 5 and 6 that the frequencies of the shell show small change when the rings number is increased from 15, as well as influence of rings on frequency in both case is similar.

Figure 7 depicts the effects of the numbers of stringer on the backward-traveling wave for the rotating stringer-stiffened conical shell. In this case, the numbers of stringers are 0, 20, and 40, and speed of rotation is 10(rev/s), where no ring is presented. It is observed that, at small circumferential wave number, influence

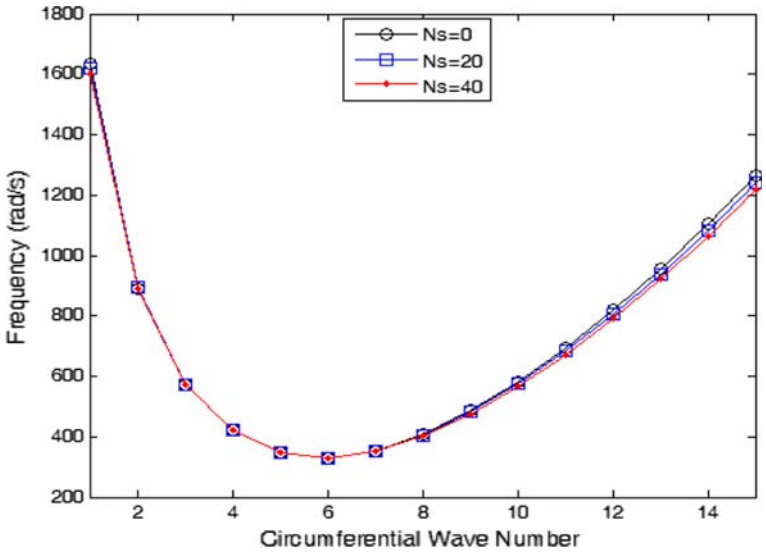

Fig. 7 Variation of the natural frequencies for the rotating and stringer stiffened composite conical shell with the circumferential wave number at various different numbers of stringers. Lamination scheme $[0°/90°/0°]$, $L/a = 8$, $h/a = 0.008$, $m = 1$, $N_r = 0$, $\Omega = 10$(rev/s), $\alpha = 15°$

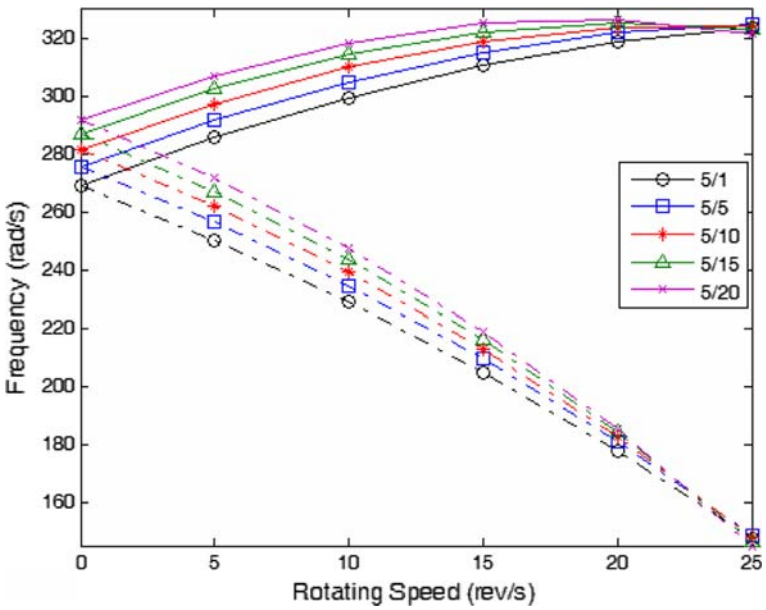

Fig. 8 Variation of the bifurcation of natural frequencies for a rotating and stiffened composite conical shell with different number of rings. Lamination scheme $[0°/90°/0°]$, $L/a = 8$, $h/a = 0.004$, $m = 1$, $n = 3$, $N_s = 5$, $\alpha = 15°$

of number of stringer is insignificant. At large circumferential wave number, just at frequencies more than fundamental frequency, the frequency will be decreased where the number of stringers is increased. There is a main difference observed between conical and cylindrical shells, comparing the effects of stringers on natural frequency, because, the radius of conical shell is increased along the axial axis and then the inertial forces of stringers are increased. Therefore, the natural frequency of the shell is decreased where as the cylindrical shell behaves in opposite way.

Figure 8 illustrates the effects of the number of rings on the frequencies of the rotating conical shells for mode (1, 3). It is observed that at small rotating speed, the frequencies of the shells generally increase with the increase of the number of the rings for both forward and backward waves. At higher speeds, the difference between natural frequency of stiffened shell and un-stiffened shell is neglected and the curves are going to

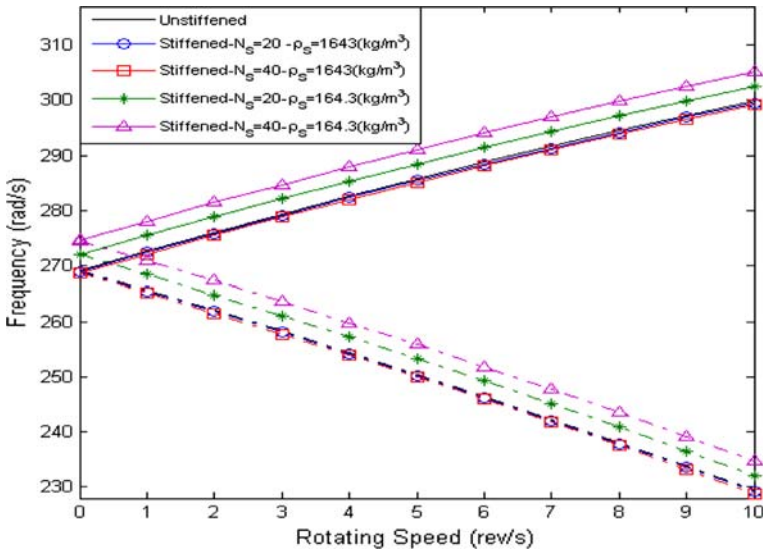

Fig. 9 Variation of the bifurcation of natural frequencies for a rotating and stiffened composite conical shell with different number of stringers. Lamination scheme $[0°/90°/0°]$, $L/a = 8$, $h/a = 0.004$, $m = 1$, $n = 3$, $N_r = 0$, $\alpha = 15°$

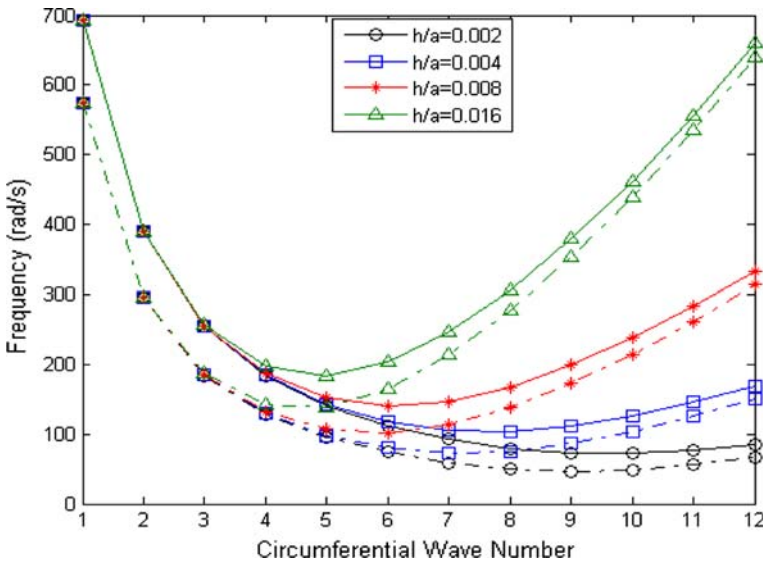

Fig. 10 Variation of the natural frequencies for the rotating and un-stiffened composite conical shell with the circumferential wave number at various different thickness of shell. Lamination scheme $[0°/90°/0°]$, $L/a = 10$, $m = 1$, $\Omega = 10$(rev/s), $\alpha = 15°$

be coincident. This is due to the fact that the inertial terms of stiffened shell are more considerable than the stiffness terms.

Figure 9 depicts the coupled effects of variation of stringer and density of stringers on the frequency characteristics. As shown in Fig. 9, when the density of stringers is equal to the density of the shell, the number of stringer has no influence on frequency characteristics. However, increasing the number of stringers, when the density of stringers is decreased without any change in stiffness, results in the increases of frequency characteristics.

In order to discuss the influence of thickness of the shell on the frequency characteristics of a rotating un-stiffened conical shell and rotating stiffened conical shell, Figs. 10 and 11 are generated. In these figures, relationship between frequency and circumferential wave numbers for the four different thicknesses is presented. From Figs. 10 and 11, it can be seen that, the influence of thickness of the shell on forward and backward wave frequency characteristic is more significant when circumferential wave number (n) is large. Also, comparing these two figures at each wave number (for example mode number 12) reveals that the influence of

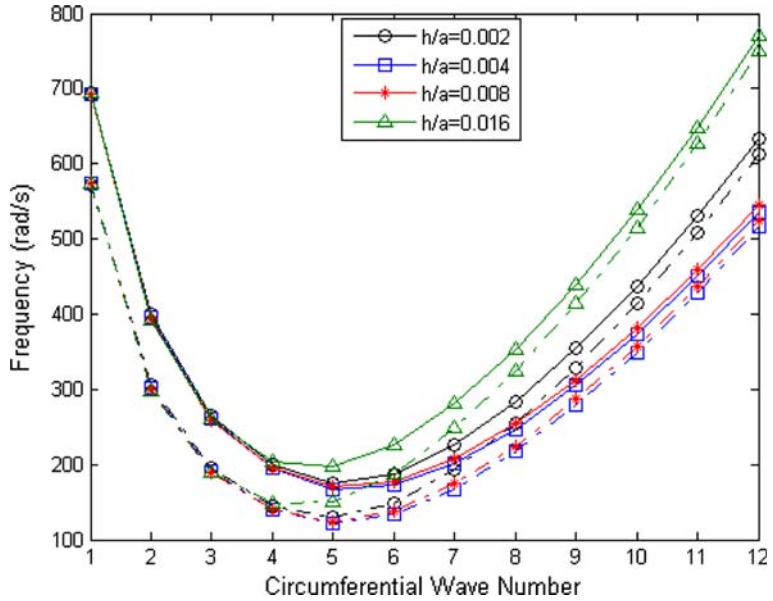

Fig. 11 Variation of the natural frequencies for the rotating and stiffened composite conical shell with the circumferential wave number at various different thickness of shell. Lamination scheme $[0°/90°/0°]$, $L/a = 10$, $m = 1$, $\Omega = 10$(rev/s), $N_s = 20$, $N_r = 10$, $\alpha = 15°$

thickness on un-stiffened shell is more considerable than on the stiffened shell. Moreover, the comparison of natural frequency of stiffened and un-stiffened shell with different shell thicknesses is another justification for using light stiffened shells in the place of heavy un-stiffened shells with the same order of natural frequencies.

4 Conclusions

The free vibration analysis of the stiffened, simply-supported, rotating cross-ply laminated conical shells has been investigated via Ritz method by treating the stiffeners as discrete elements. The eigenvalue equation results have been validated by comparing with the previously published results for the non-rotating conical shell without stiffener and the orthogonally stiffened rotating composite cylindrical shells.

Generally, using the ring stiffeners in construction of low rotating speed conical shell lead to increase of natural frequency. However, the effect of stringers on natural frequency depends on stiffener density and rotating speed of the shell. In addition, as anticipated, the increase in shell thickness leads to increase of natural frequency, but this effect for stiffened shell is not considerable.

Appendix A

$$
\begin{aligned}
L_{11} = {} & \left(\rho h\omega^2 + \rho h\Omega^2 S_\alpha^2 - A_{11}\lambda^2\right)\left[\frac{1}{2\pi}L(2aS_\alpha\pi^2 + \pi^2 L)\right] - \left(A_{22}S_\alpha^2 + A_{66}n^2\right)\int_0^{2\pi}\int_0^{L}\frac{C_x^2}{r^2(x)}\mathrm{d}x\mathrm{d}\theta \\
& + \left[\rho_s A_s N_s\left(\Omega^2 S_\alpha^2 + \omega^2\right) - E_s N_s A_s\lambda^2\right]\int_0^{2\pi}\int_0^{L} C_x^2\mathrm{d}x\mathrm{d}\theta + \int_0^{2\pi}\left(\rho_r A_r\left(\Omega^2 S_\alpha^2 + \omega^2\right)\sum_{K=1}^{N_r} r(x_K)C_k^2\right)\mathrm{d}\theta \\
& - \int_0^{2\pi}\left(A_r E_r S_\alpha^2\sum_{K=1}^{N_r}\frac{C_k^2}{r(x_k)}\right) - \rho h\Omega^2 S_\alpha^2\int_0^{2\pi}\int_0^{L} r(x)C_x^2\mathrm{d}x\mathrm{d}\theta - \rho_r A_r\Omega^2 S_\alpha^2\sum_{K=1}^{N_r} r(x_K)C_k^2 \qquad \text{(A1)}
\end{aligned}
$$

where $\lambda = m\pi/L$, $S_\alpha = \sin\alpha$, $C_\alpha = \cos\alpha$, $S_x = \sin(\lambda x)$, $C_x = \cos(\lambda x)$, $S_k = \sin(\lambda x_k)$, $C_k = \cos(\lambda x_k)$.

$$L_{12} = 2\rho h\Omega\omega S_\alpha \int_0^{2\pi}\int_0^{L} r(x)S_xC_x\mathrm{d}x\mathrm{d}\theta - [A_{22}+A_{66}]nS_\alpha \int_0^{2\pi}\int_0^{L} \frac{S_xC_x}{r(x)}\mathrm{d}x\mathrm{d}\theta + [A_{66}+A_{12}]\lambda n \times \int_0^{L} C_x^2\mathrm{d}x + 2\rho_s N_s A_s \Omega\omega S_\alpha \int_0^{2\pi}\int_0^{L} S_xC_x\mathrm{d}x\mathrm{d}\theta + 4\pi\rho_r A_r \Omega\omega S_\alpha \sum_{K=1}^{N_r} r_k S_k C_k - 2\pi A_r E_r n S_\alpha \times \sum_{K=1}^{N_r} \frac{S_kC_k}{r_k} - 2\pi\rho h\Omega^2 n S_\alpha \int_0^{L} r(x)S_xC_x\mathrm{d}x - 2\pi A_r\Omega^2 n S_\alpha \sum_{K=1}^{N_r} r(x_k)S_kC_k \tag{A2}$$

$$L_{13} = 2\pi\rho h\Omega^2 C_\alpha S_\alpha \int_0^{L} r(x)S_xC_x\mathrm{d}x - A_{22}C_\alpha S_\alpha \int_0^{2\pi}\int_0^{L} \frac{S_xC_x}{r(x)}\mathrm{d}x\mathrm{d}\theta + 2A_{12}\pi\lambda C_\alpha \times \int_0^{L} C_x^2\mathrm{d}x - \rho_s N_s A_s\left(Z_s\lambda\omega^2 + \Omega^2 Z\lambda S_\alpha^2\right)\int_0^{L} C_x^2\mathrm{d}x + \rho_s N_s A_s(\Omega^2 C_\alpha S_\alpha) \times \int_0^{L} S_xC_x\mathrm{d}x + 2\rho_s N_s A_s\Omega\omega n Z S_\alpha \int_0^{L} \frac{S_xC_x}{r(x)}\mathrm{d}x + E_s N_s A_s Z\lambda^3 \int_0^{L} C_x^2\mathrm{d}x - 2\pi\rho_r A_r\left(Z_r\lambda\omega^2 + \Omega^2 Z_r\lambda S_\alpha^2\right) \times \sum_{K=1}^{N_r} r(x_k)C_k^2 + 2\pi\rho_r A_r\left(\Omega^2 S_\alpha C_\alpha\right)\sum_{K=1}^{N_r} r(x_k)S_kC_k + 4\pi\rho_r A_r\Omega\omega n Z_r S_\alpha \times \sum_{K=1}^{N_r} S_kC_k - 2\pi A_r E_r Z_r n^2 S_\alpha \sum_{K=1}^{N_r} \frac{S_kC_k}{r^2(x_k)} + 2\pi A_r E_r Z_r\lambda S_\alpha^2 \times \sum_{K=1}^{N_r} \frac{C_k^2}{r(x_k)} - 2\pi A_r E_r C_\alpha S_\alpha \sum_{K=1}^{N_r} \frac{S_kC_k}{r(x_k)} - 2\pi\rho h\Omega^2 C_\alpha S_\alpha \int_0^{L} r(x)C_xS_x\mathrm{d}x - 2\pi\rho_r A_r Z_r\Omega^2 n^2 S_\alpha \times \sum_{K=1}^{N_r} S_kC_k + 2\pi\rho_r A_r Z_r\Omega^2 S_\alpha^2 \sum_{K=1}^{N_r} r(x_k)C_k^2 - 2\pi\rho_r A_r\Omega^2 C_\alpha S_\alpha \sum_{K=1}^{N_r} r(x_k)C_kS_k \tag{A3}$$

$$L_{21} = 4\pi\rho h\Omega\omega S_\alpha \int_0^{L} r(x)S_xC_x\mathrm{d}x - 2[A_{22}+A_{66}]\pi n S_\alpha \int_0^{L} \frac{S_xC_x}{r(x)}\mathrm{d}x + 2[A_{66}+A_{12}]\pi\lambda n \times \int_0^{L} C_x^2\mathrm{d}x + 2\rho_s N_s A_s\Omega\omega S_\alpha \int_0^{L} S_xC_x\mathrm{d}x + 4\pi\rho_r A_r\Omega\omega S_\alpha \sum_{K=1}^{N_r} r_kS_kC_k - 2\pi A_r E_r n S_\alpha \times \sum_{K=1}^{N_r} \frac{S_kC_k}{r(x_k)} - 2\pi\rho h\Omega^2 n S_\alpha \int_0^{L} r(x)S_xC_x\mathrm{d}x - 2\pi\rho_r A_r\Omega^2 n S_\alpha \sum_{K=1}^{N_r} r(x_k)S_kC_k \tag{A4}$$

$$L_{22} = 2\rho h\pi(\omega^2+\Omega^2)\int_0^L r(x)S_x^2\mathrm{d}x - 2\pi(A_{22}n^2 + A_{66}S_\alpha^2 + 4D_{66}\lambda^2C_\alpha^2)$$
$$\times\int_0^L \frac{S_x^2}{r(x)}\mathrm{d}x - 2\pi(D_{22}n^2C_\alpha^2 + 4D_{66}S_\alpha^2C_\alpha^2)\int_0^L \frac{S_x^2}{r^3(x)}\mathrm{d}x - A_{66}\lambda^2\int_0^L r(x)S_x^2\mathrm{d}x + \rho_sN_sA_s(\omega^2+\Omega^2)$$
$$\times\int_0^L S_x^2\mathrm{d}x + 2\pi\rho_rA_r(\omega^2+\Omega^2)\sum_{K=1}^{N_r} r(x_k)S_k^2 - 2\pi A_rE_rn^2$$
$$\times\sum_{K=1}^{N_r}\frac{S_k^2}{r(x_k)} - 2\pi\rho\Omega^2n^2\left(h\int_0^L r(x)S_x^2\mathrm{d}x + A_r\sum_{K=1}^{N_r} r(x_k)S_k^2\right) \tag{A5}$$

$$L_{23} = 4\pi\rho h\Omega\omega C_\alpha\int_0^L r(x)S_x^2\mathrm{d}x - 2\pi C_\alpha(A_{22}n + 4D_{66}\lambda^2n + D_{12}\lambda^2n)$$
$$\times\int_0^L \frac{S_x^2}{r(x)}\mathrm{d}x - 2\pi C_\alpha(4D_{66}nS_\alpha^2 + D_{22}n^3)\int_0^L \frac{S_x^2}{r^3(x)}\mathrm{d}x + 2\pi D_{22}\lambda nS_\alpha C_\alpha$$
$$\times\int_0^L \frac{C_xS_x}{r^2(x)}\mathrm{d}x - 2\rho_sN_sA_s\Omega Z_s\lambda\omega\int_0^L C_xS_x\mathrm{d}x + 2\rho_sN_sA_s\Omega\omega C_\alpha$$
$$\times\int_0^L S_x^2\mathrm{d}x + \rho_sN_sA_sZ_sn\left(\omega^2+\Omega^2\right)\int_0^L \frac{S_x^2}{r(x)}\mathrm{d}x - 4\pi\rho_rA_r\Omega Z_r\lambda\omega S_\alpha$$
$$\times\sum_{K=1}^{Nr} r(x_k)C_kS_k + 4\pi\rho_rA_r\Omega\omega C_\alpha\sum_{K=1}^{Nr} r(x_k)S_k^2 + 2\pi\rho_rA_rZ_rn(\omega^2+\Omega^2)$$
$$\times\sum_{K=1}^{N_r} S_k^2 + 2\pi A_rE_rnC_\alpha\int_0^L \frac{S_k^2}{r(x)}\mathrm{d}x + 2\pi A_rE_rn^3Z_r\int_0^L \frac{S_k^2}{r^2(x)}\mathrm{d}x + 2\pi A_rE_rZ_r\lambda nS_\alpha$$
$$\times\sum_{K=1}^{N_r}\frac{C_kS_k}{r(x_k)} - 2\pi\rho h\Omega^2nC_\alpha\int_0^L r(x)S_x^2\mathrm{d}x + 2\pi\rho A_r\Omega^2Z_r\lambda nS_\alpha\sum_{K=1}^{Nr} r(x_k)C_kS_k - 2\pi\rho_rA_r\Omega^2nC_\alpha$$
$$\times\sum_{K=1}^{N_r} r(x_k)S_k^2 - 2\pi\rho_rA_r\Omega^2n^3\sum_{K=1}^{N_r} S_k^2 \tag{A6}$$

$$L_{31} = 2\pi\rho h\Omega^2C_\alpha S_\alpha\int_0^L r(x)S_xC_x\mathrm{d}x - A_{22}C_\alpha S_\alpha\int_0^L \frac{S_xC_x}{r(x)}\mathrm{d}x + 2A_{12}\pi\lambda C_\alpha$$
$$\times\int_0^L S_x^2\mathrm{d}x - \rho_sN_sA_s(Z_s\lambda\omega^2 + \Omega^2Z\lambda S_\alpha^2)\int_0^L S_x^2\mathrm{d}x + \rho_sN_sA_s\left(\Omega^2C_\alpha S_\alpha\right)$$

$$\times \int_0^L S_x C_x \mathrm{d}x - 2\rho_s N_s A_s \Omega\omega n Z S_\alpha \int_0^L \frac{S_x C_x}{r(x)}\mathrm{d}x + E_s N_s A_s Z_s \lambda^3$$
$$\times \int_0^L S_x^2 \mathrm{d}x - 2\pi\rho_r A_r \left(Z_r \lambda\omega^2 + \Omega^2 Z_r \lambda S_\alpha^2\right) \sum_{K=1}^{N_r} r(x_k) S_k^2 + 2\pi\rho_r A_r (\Omega^2 S_\alpha C_\alpha)$$
$$\times \sum_{K=1}^{N_r} r(x_k) S_k C_k - 4\pi\rho_r A_r \Omega\omega n Z_r S_\alpha \sum_{K=1}^{N_r} S_k C_k - 2\pi A_r E_r Z_r n^2 S_\alpha \sum_{K=1}^{N_r} \frac{S_k C_k}{r^2(x_k)} + 2\pi A_r E_r Z_r \lambda S_\alpha^2$$
$$\times \sum_{K=1}^{N_r} \frac{S_k^2}{r(x_k)} - 2\pi A_r E_r C_\alpha S_\alpha \sum_{K=1}^{N_r} \frac{S_k C_k}{r(x_k)} - 2\pi\rho h \Omega^2 C_\alpha S_\alpha \int_0^L r(x) C_x S_x \mathrm{d}x - 2\pi\rho_r A_r Z_r \Omega^2 n^2 S_\alpha$$
$$\times \sum_{K=1}^{N_r} S_k C_k + 2\pi\rho_r A_r Z_r \Omega^2 S_\alpha^2 \sum_{K=1}^{N_r} r(x_k) S_k^2 - 2\pi\rho_r A_r \Omega^2 C_\alpha S_\alpha \sum_{K=1}^{N_r} r(x_k) C_k S_k \tag{A7}$$

$$L_{32} = 4\pi\rho h \Omega\omega C_\alpha \int_0^L r(x) S_x^2 \mathrm{d}x - 2\pi C_\alpha \Bigg(\left(A_{22} n + 4D_{66}\lambda^2 n + D_{12}\lambda^2 n\right)$$
$$\times \int_0^L \frac{S_x^2}{r(x)}\mathrm{d}x + \left(4D_{66} n S_\alpha^2 + D_{22} n^3\right) \int_0^L \frac{S_x^2}{r^3(x)}\mathrm{d}x \Bigg)$$
$$-2\pi D_{22}\lambda n S_\alpha C_\alpha \int_0^L \frac{C_x S_x}{r^2(x)}\mathrm{d}x + 2\rho_s N_s A_s \Omega\omega \left(Z_s \lambda S_\alpha \int_0^L C_x S_x \mathrm{d}x + C_\alpha \int_0^L S_x^2 \mathrm{d}x \right)$$
$$+ \rho_s N_s A_s Z_s n \left(\omega^2 + \Omega^2\right) \int_0^L \frac{S_x^2}{r(x)}\mathrm{d}x + 4\pi\rho_r A_r \Omega\omega \left(Z_r \lambda S_\alpha \sum_{K=1}^{Nr} r(x_k) C_k S_k + C_\alpha \sum_{K=1}^{Nr} r(x_k) S_k^2 \right)$$
$$+ 2\pi\rho_r A_r Z_r n(\omega^2 + \Omega^2) \sum_{K=1}^{N_r} S_k^2 - 2\pi A_r E_r n C_\alpha \sum_{K=1}^{N_r} \frac{S_k^2}{r(x_k)}$$
$$- 2\pi A_r E_r \left(n^3 Z_r \sum_{K=1}^{N_r} \frac{S_k^2}{r^2(x_k)} + Z_r \lambda n S_\alpha \sum_{K=1}^{N_r} \frac{C_k S_k}{r(x_k)} \right) - 2\pi\rho h \Omega^2 n C_\alpha \int_0^L r(x) S_x^2 \mathrm{d}x$$
$$-2\pi\rho_r A_r \Omega^2 \left(Z_r \lambda n S_\alpha \sum_{K=1}^{Nr} r(x_k) C_k S_k + n C_\alpha \sum_{K=1}^{N_r} r(x_k) S_k^2 + n^3 \sum_{K=1}^{N_r} S_k^2 \right) \tag{A8}$$

$$L_{33} = 2\pi\rho h \left(\Omega^2 C_\alpha^2 + \omega^2\right) \int_0^L r(x) S_x^2 \mathrm{d}x - 2\pi (A_{22} C_\alpha^2 + D_{22} S_\alpha^2 \lambda^2 + 4D_{66}\lambda^2 n^2 + 2D_{12}\lambda^2 n^2)$$
$$\times \int_0^L \frac{S_x^2}{r(x)}\mathrm{d}x - 2\pi \left(D_{22} n^4 + 4D_{66} n^2 S_\alpha^2\right) \int_0^L \frac{S_x^2}{r^3(x)}\mathrm{d}x - 2\pi D_{11}\lambda^4$$
$$\times \int_0^L r(x) S_x^2 \mathrm{d}x + \rho_s N_s (I_{os}\lambda^2\omega^2 + A_s\omega^2 + A_s\Omega^2 C_\alpha^2 + \Omega^2 I_{os}\lambda^2 S_\alpha)$$

$$\times \int_0^L S_x^2 \mathrm{d}x + \rho_s N_s I_{os} n^2 \left(\omega^2 + \Omega^2\right) \int_0^L \frac{S_x^2}{r^2(x)} \mathrm{d}x + 4\rho_s A_s N_s Z_s n \Omega \omega \int_0^L \frac{S_x^2}{r(x)} \mathrm{d}x - E_s N_s I_{os} \lambda^4$$

$$\times \int_0^L S_x^2 \mathrm{d}x - G_s J_s N_s n^2 \lambda^2 \int_0^L \frac{S_x^2}{r^2(x)} \mathrm{d}x + 2\pi\rho_r \left(I_{or}\lambda^2\omega^2 + A_r\omega^2 + A_r\Omega^2 C_\alpha^2 + \Omega^2 I_{or}\lambda^2 S_\alpha\right)$$

$$\times \sum_{K=1}^{N_r} r(x_k) S_k^2 + 2\pi\rho_r I_{or} n^2 (\omega^2 + \Omega^2) \sum_{K=1}^{N_r} \frac{S_k^2}{r^2(x_k)} + 8\pi\rho_r A_r Z_r n \Omega \omega C_\alpha$$

$$\times \sum_{K=1}^{N_r} S_k^2 - 2\pi A_r E_r \left(Z_r^2 \lambda^2 S_\alpha^2 + C_\alpha^2\right) \sum_{K=1}^{N_r} \frac{S_k^2}{r(x_k)} - 2\pi E_r I_{or} n^4 \sum_{K=1}^{N_r} \frac{S_k^2}{r^3(x_k)} + 4\pi A_r E_r Z_r n^2 C_\alpha$$

$$\times \sum_{K=1}^{N_r} \frac{S_k^2}{r^2(x_k)} + 2\pi G_r J_r \lambda^2 n^2 \sum_{K=1}^{N_r} \frac{S_k^2}{r(x_k)} - 2\pi\rho h \Omega^2 C_\alpha^2 \int_0^L r(x) S_x^2 \mathrm{d}x$$

$$- 4\pi\rho_r A_r Z_r n^2 \Omega^2 C_\alpha \sum_{K=1}^{N_r} S_k^2 - 2\pi\rho_r I_{or} n^4 \Omega^2 \sum_{K=1}^{N_r} \frac{S_k^2}{r(x_k)} - 2\pi\rho_r \Omega^2 (I_{or}\lambda^2 S_\alpha^2 + A_r C_\alpha^2) \sum_{K=1}^{N_r} r(x_k) S_k^2 \tag{A9}$$

where $I_{os} = I_s + Z_s^2 A_s$, $I_{or} = I_r + Z_r^2 A_r$. I_s and I_r are the moments of inertia of the stringers and rings about their centroidal axes, respectively, and the respective polar moments of inertia are

$$J_s = \frac{1}{3} b_s h_s^3,\ J_r = \frac{1}{3} b_r h_r^3$$

References

1. Leissa, A.W.: Vibration of shells. NASA. SP-288 (1973)
2. Soedel, W.: Vibrations of Shells and Plates, Revised and Expanded, 2nd edn. Marcel Dekker, New York (1996)
3. Reddy, J.N.: Mechanics of Laminated Composite Plates and Shells: Theory and Analysis, 2nd edn. CRC press, New York (2004)
4. Chen, Y., Zhao, H.B., Shea, Z.P.: Vibrations of high speed rotating shells with calculations for cylindrical shells. J. Sound Vib. **160**, 137–160 (1993)
5. Lam, K.Y., Loy, C.T.: On vibrations of thin rotating laminated composite cylindrical shells. Compos. Eng. **4**, 1153–1167 (1994)
6. Lam, K.Y., Loy, C.T.: Free vibrations of a rotating multi-layered cylindrical shell. Int. J. Solids Struct. **32**, 647–663 (1995)
7. Lam, K.Y., Loy, C.T.: Analysis of rotating laminated cylindrical shells by different thin shell theories. J. Sound Vib. **186**, 23–25 (1995)
8. Hua, L., Lam, K.Y.: Frequency characteristics of a thin rotating cylindrical shell using the generalized differential quadrature method. Int. J. Mech. Sci. **40**, 443–459 (1998)
9. Lam, K.Y., Hua, L.: Vibration analysis of a rotating truncated circular conical shell. Int. J. Solids Struct. **34**(17), 2183–2197 (1997)
10. Zhao, X., Liew, K.M., Ng, T.Y.: Vibration of rotating cross-ply laminated circular cylindrical shells with stringer and ring stiffeners. Int. J. Solids Struct. **39**, 529–545 (2002)
11. Jafari, A.A., Bagheri, M.: Free vibration of rotating ring stiffened cylindrical shells with non-uniform stiffener distribution. J. Sound Vib. **296**, 353–376 (2006)
12. Lim, C.W., Liew, K.M.: Vibratory behaviour of shallow conical shells by a global Ritz formulation. Eng. Struct. **17**(1), 63–70 (1995)
13. Rao, S.S.: Vibration of Continuous Systems. Wiley, London (2007)
14. Lam, K.Y., Hua, L.: Influence of boundary conditions on the frequency characteristics of a rotating truncated circular conical shell. J. Sound Vib. **223**(2), 171–195 (1999)